Discontinuous Galerkin Methods for the Chemotaxis and Haptotaxis Models

Yekaterina Epshteyn [1]

Department of Mathematical Sciences, Carnegie Mellon University, Pittsburgh, PA, 15213, rina10@andrew.cmu.edu

Abstract

In this work, first we formulate and compare three different discontinuous Interior Penalty Galerkin methods for the two-dimensional Keller-Segel chemotaxis model. Keller-Segel chemotaxis model is the important starting step in the modeling of the real biological system. We show in the numerical tests that two of the proposed methods fail to give accurate, oscillation-free solutions.

Next, we consider the application of the successful method for the Keller-Segel model to the simulation of the more realistic, and closely related haptotaxis model of tumor invasion into healthy tissues.

Key words: Keller-Segel chemotaxis model, haptotaxis model, convection-diffusion-reaction systems, discontinuous Galerkin methods, NIPG, IIPG, and SIPG methods, Cartesian meshes.

1 Introduction

Since the late nineties, the discontinuous Galerkin (DG) methods have been successfully applied to a wide variety of problems, ranging from solid mechanics to fluid mechanics (see, e.g., [2,5,13,14,16,21,23,36]). Among the attractive features of DG are local, element-wise mass conservation, flexibility to use high-order polynomial and non-polynomial basis functions, ability to easily increase the order of approximation on each mesh element independently, and to achieve an almost exponential convergence rate when smooth solutions are captured on appropriate meshes. Also worth mentioning are block diagonal

[1] The research of Y.Epshteyn is based upon work supported by the Center for Nonlinear Analysis (CNA) under the National Science Foundation Grant # DMS-0635983.

mass matrices, which are of great computational advantage if an explicit time integration is used with DG.

In this paper, we first consider the most common formulation of the Keller-Segel system [12], which can be written in the dimensionless form as

$$\begin{cases} \rho_t + \nabla \cdot (\chi \rho \nabla c) = \Delta \rho, \\ c_t = \Delta c - c + \rho, \end{cases} \quad (x, y) \in \Omega, t > 0, \tag{1}$$

subject to the Neumann boundary conditions:

$$\nabla \rho \cdot \mathbf{n} = \nabla c \cdot \mathbf{n} = 0, \quad (x, y) \in \partial\Omega, \tag{2}$$

where Ω is a bounded domain in $\mathbb{R}^2$, $\partial\Omega$ is its boundary and $\mathbf{n}$ is a unit normal vector. We also have the following variables:

- $\rho(x, y, t)$ is the cell density,
- $c(x, y, t)$ is the chemoattractant concentration, and
- χ is a chemotactic sensitivity constant.

It is well-known that solutions of the system (1) may blow up in finite time (see [25,26]). This blow-up is a mathematical description of a cell concentration phenomenon that occurs in real biological systems (see [1,6–8,15,32]). The Keller-Segel model (1) can be generalized to better reproduce the reality by taking into account several additional factors, such as growth and death of cells, presence of different chemicals in the biological system.

A common property of all existing chemotaxis systems is their ability to model a concentration phenomenon, which mathematically results in solutions rapidly growing in small neighborhoods of concentration points or curves. The solutions may blow up or may exhibit a very singular behavior.

Capturing such singular solutions numerically is a challenging problem. A few numerical methods have been proposed (see [22],[31]), for a simpler version of the Keller-Segel model,

$$\begin{cases} \rho_t + \nabla \cdot (\chi \rho \nabla c) = \Delta \rho, \\ \Delta c - c + \rho = 0, \end{cases}$$

Here the equation for concentration c has been replaced by an elliptic equation, using an assumption that the chemoattractant concentration c changes over much smaller time scales than the density ρ. A fractional step numerical method for a fully time-dependent chemotaxis system from [37] has been proposed in [38]. However, the operator splitting approach may not be applicable when a convective part of the chemotaxis system is not hyperbolic, which is a

generic situation for the original Keller-Segel model. This was shown in [11] by introducing new variables for $(u, v) := \nabla c$. In [11], the finite-volume Godunov-type central-upwind scheme was derived for (1) and extended to some other chemotaxis and haptotaxis models. As it was mentioned above, the starting points in the derivation of the central-upwind scheme in [11] were introduction of new variables $(u, v) := (c_x, c_y)$, differentiation of the concentration equation in (1) with respect to x and y, and rewriting of the original system in an equivalent form. In this new form. the concentration equation is replaced with the corresponding equation for the u, v :

$$\begin{aligned} \rho_t + (\chi\rho u)_x + (\chi\rho v)_y &= \Delta\rho, \\ u_t - \rho_x &= \Delta u - u, \\ v_t - \rho_y &= \Delta v - v \end{aligned} \tag{3}$$

The system (3) is an appropriate form of the chemotaxis system if one wants to solve it numerically by a finite-volume method. Even though the convective part of the system (3) is not hyperbolic (see [11]), some stability of the resulting central-upwind scheme was ensured by proving its positivity preserving property (see [11]).

A major disadvantage of the system (3) is a mixed type of its convective part. Especially, when a higher order numerical method is applied to (3), a transition in the numerical scheme from a hyperbolic region to an elliptic one may cause severe instabilities in the solution since the wave propagation speeds in the elliptic region are infinite. Therefore, in order to develop high-order DG methods for (1), we wrote it in a different form which is suitable for discontinuous Galerkin settings (see [19]):
Let $(u, v) := (c_x, c_y)$,

$$\rho_t + (\chi\rho u)_x + (\chi\rho v)_y = \Delta\rho, \tag{4}$$
$$c_t = \Delta c - c + \rho, \tag{5}$$
$$c_x = u, \tag{6}$$
$$c_y = v, \tag{7}$$

where the new unknowns ρ, c, u, v satisfy the following boundary conditions:

$$\nabla\rho \cdot \mathbf{n} = \nabla c \cdot \mathbf{n} = (u, v)^T \cdot \mathbf{n} = 0, \quad (x, y) \in \partial\Omega. \tag{8}$$

The convective part of the system (4)-(7) is hyperbolic. In [19], for the obtained system (4)-(7), we developed a family of high-order DG methods. The proposed methods are based on three primal discontinuous Galerkin methods: Nonsymmetric Interior Penalty Galerkin (NIPG), Symmetric Interior Penalty Galerkin (SIPG), and Incomplete Interior Penalty Galerkin (IIPG) methods [4,17,18,35]. The choice of the numerical fluxes is crucial for the stability of any scheme. The reader may consult, for more details, a study of DG numerical fluxes (based on various approximate of Riemann problem solver) for the

nonlinear conservation laws (see [34]) and a study of the diffusive numerical fluxes for DG schemes for linear transport equation (see [33]).

The numerical fluxes for the approximation of the convective terms in the proposed DG methods are based on the techniques for the semidiscrete finite-volume central-upwind schemes developed in [29] (see also [28], [30]). These schemes belong to the family of nonoscillatory central schemes, which are highly accurate, efficient, applicable to general multidimensional systems of conservation laws and related problems. Like other central fluxes, the central-upwind ones are obtained without using (an approximate) Riemann problem solver, which is unavailable for the systems under consideration. At the same time, a certain upwinding information—one-sided speeds of propagation—is incorporated into the central-upwind fluxes.

In [19] we considered Cartesian grids, and for the proposed high-order DG methods we proved the error estimates under the assumption of boundedness of the exact solution. We also showed an interesting result that the blow-up time of the exact solution is bounded from above by the blow-up time of the solution of DG methods. In numerical tests presented in [19], we demonstrated that the obtained numerical solutions have no negative values, and are oscillation-free even without application of the slope limiting techniques.

In this paper, we would like first to compare three different discontinuous Galerkin schemes applied to the classical Keller-Segel model:

- primal discontinuous Galerkin method applied to the original formulation of the Keller-Segel model (1)
- primal discontinuous Galerkin method with the standard upwind numerical fluxes for the reformulated Keller-Segel model (4)-(7)
- the new discontinuous Galerkin method developed in [19].

In the numerical tests in Section (4), we first show that compared to the new discontinuous Galerkin method, the first two schemes fail to give the accurate oscillation free solutions for the classical Keller-Segel chemotaxis model.

Secondly, we consider the important application of the new discontinuous Galerkin scheme to the simulation of the more realistic, and closely related, haptotaxis model of the tumor invasion (cancerous cell migration) into healthy tissue.

The paper is organized as follows. In §2, we introduce the notations. In section §3-§4, we formulate different discontinuous Galerkin methods applied to Keller-Segel model of the chemotaxis and show the numerical results. Finally in section §5, we present the new discontinuous Galerkin methods applied to the simulation of the haptotaxis model and give some conclusions.

2 Notations

We consider a discontinuous finite element discretization of the chemotaxis Keller-Segel model and closely related haptotaxis model below. For this we introduce a non-degenerate subdivision of the domain Ω, made of rectangles and denoted by $\mathcal{E}_h$. As usual, the maximum diameter over all mesh elements is denoted by h. The set of interior edges is denoted by Γ_h. To each edge e in Γ_h, we associate a unit normal vector $\mathbf{n}_e = (\mathbf{n}_x, \mathbf{n}_y)$, with x-coordinate $\mathbf{n}_x$ and y-coordinate $\mathbf{n}_y$. We assume that $\mathbf{n}_e$ is directed from the E^1 to E^2 (where E^1 denotes the element with smaller index and E^2 denotes the element with larger index). For a boundary edge, $\mathbf{n}_e$ is chosen so that it coincides with the outward normal. The discrete space of discontinuous piecewise polynomials of degree r is denoted by $\mathcal{W}_{r,h}$:

$$\mathcal{W}_{r,h} = \left\{ v \in L^2(\Omega) : \forall E \in \mathcal{E}_h : v|_E \in \mathrm{P}_r(E) \right\}$$

For any function $v \in \mathcal{W}_{r,h}$, we denote the jump and average operator over given edge e by $[v]$ and $\{v\}$ respectively. Assuming that $\mathbf{n}_e$ is outward to E^1, we can write:

$$\forall e = \partial E_e^1 \cap \partial E_e^2, \quad [v]|_e = v|_{E_e^1} - v|_{E_e^2}, \quad \{v\}|_e = 0.5v|_{E_e^1} + 0.5v|_{E_e^2},$$

$$\forall e = \partial E_e^1 \cap \partial\Omega, \quad [v]|_e = v|_{E_e^1}, \quad \{v\}|_e = v|_{E_e^1}.$$

We also denote by Ω a rectangular domain with the boundary $\partial\Omega = \partial\Omega_1 \cup \partial\Omega_2$, where $\partial\Omega_1$ and $\partial\Omega_2$ are the vertical and horizontal pieces of the boundary $\partial\Omega$, respectively.

3 Description of the numerical schemes for classical Keller-Segel chemotaxis model

We first consider the original Keller-Segel system of equations (1)-(2). Before formulating the scheme, we introduce some additional notation. Let ε be a parameter that takes the value $-1, 0$ or 1. By changing the value of ε, we will obtain the SIPG, IIPG or NIPG method. Let $\sigma_\rho, \sigma_c, \sigma_u$ and σ_v be positive real parameters, called penalty parameters. Stability of NIPG method does not depend on the choice of the penalty parameters. However, the penalty parameters have to be bounded below by a large enough constant (depending on the problem), to ensure the stability of SIPG and IIPG. For the general idea on how to estimate the penalty parameters for SIPG (similar techniques can be used for IIPG), see for example [20]. By r_ρ, r_c, r_u and r_v we denote the degree of the polynomial approximations for ρ, c, u and v respectively.

The direct application of the Interior Penalty Galerkin Methods to (1)-(2) yields the following semi-discrete scheme.

Scheme 1.

Find $(\rho^{DG}, c^{DG}) \in H^1([0,T]) \cap \mathcal{W}^{\rho}_{r_\rho,h} \times \mathcal{W}^{c}_{r_c,h}$ such that:

$$\int_\Omega \rho_t^{DG} w^\rho + \sum_{E\in\mathcal{E}_h} \int_E (\nabla\rho^{DG} - \chi\rho^{DG}\nabla c^{DG})\nabla w^\rho - \sum_{e\in\Gamma_h} \int_e \{\nabla\rho^{DG}\cdot n_e\}[w^\rho]$$

$$+\varepsilon \sum_{e\in\Gamma_h} \int_{e\in\Gamma_h} \{\nabla w^\rho \cdot n_e\}[\rho^{DG}] + \sum_{e\in\Gamma_h} \int_e \chi\rho^{DG\uparrow}\nabla c^{DG}\cdot n_e [w^\rho] + \sigma_\rho \sum_{e\in\Gamma_h} \frac{r_\rho^2}{|e|}\int_e [\rho^{DG}][w^\rho] = 0, \tag{9}$$

$$\forall w^\rho \in \mathcal{W}^{\rho}_{r_\rho,h}$$

$$\int_\Omega c_t^{DG} w^c + \int_\Omega (c^{DG} - \rho^{DG}) w^c + \sum_{E\in\mathcal{E}_h} \int_E \nabla c^{DG}\nabla w^c - \sum_{e\in\Gamma_h} \int_e \{\nabla c^{DG}\cdot n_e\}[w^c]$$

$$+\varepsilon \sum_{e\in\Gamma_h} \int_{e\in\Gamma_h} \{\nabla w^c \cdot n_e\}[c^{DG}] + \sigma_c \sum_{e\in\Gamma_h} \frac{r_c^2}{|e|}\int_e [c^{DG}][w^c] = 0, \quad \forall w^c \in \mathcal{W}^{c}_{r_c,h}, \tag{10}$$

where the the upwind value $\rho^{DG\uparrow}|_e$ defined in the standard way:

$$\rho^{DG\uparrow} = \begin{cases} \rho^{DG}|_{E_1} \text{ if } \nabla c^{DG}\cdot n_e \geq 0, \\ \rho^{DG}|_{E_2} \text{ if } \nabla c^{DG}\cdot n_e < 0. \end{cases},$$

and the initial conditions:

$$\int\limits_\Omega \rho^{\mathrm{DG}}(\cdot,0) w^\rho = \int\limits_\Omega \rho(\cdot,0) w^\rho, \quad \int\limits_\Omega c^{\mathrm{DG}}(\cdot,0) w^c = \int\limits_\Omega c(\cdot,0) w^c. \tag{11}$$

As we mentioned in the introduction of the paper, the original Keller-Segel system is of mixed elliptic-hyperbolic type. The propagation speeds in the elliptic region are infinite. Hence, the direct application of the numerical method (without separation of the elliptic and hyperbolic region in the convective term of the numerical scheme) can cause severe instabilities in the solution, which will be demonstrated in Section (4) for the scheme (9)-(10).

Next, consider (4)-(7) subject to (8). The system (4)-(7) is the system of convection-diffusion-reaction equations

$$k\mathbf{Q}_t + \mathbf{F}(\mathbf{Q})_x + \mathbf{G}(\mathbf{Q})_y = k\Delta\mathbf{Q} + \mathbf{R}(\mathbf{Q}), \tag{12}$$

where $\mathbf{Q} := (\rho, c, u, v)^T$, the fluxes are $\mathbf{F}(\mathbf{Q}) := (\chi\rho u, 0, c, 0)^T$ and $\mathbf{G}(\mathbf{Q}) := (\chi\rho v, 0, 0, c)^T$ and the reaction term is $\mathbf{R}(\mathbf{Q}) := (0, \rho - c, u, v)$. Also, the constant $k = 1$ in the first two equations in (12), and $k = 0$ in the third and

the fourth equations. Here, the Jacobian of $\mathbf{F}$ and $\mathbf{G}$ has only real eigenvalues given below:

$$\lambda_1^{\mathbf{F}} = \chi u,\ \lambda_2^{\mathbf{F}} = \lambda_3^{\mathbf{F}} = \lambda_4^{\mathbf{F}} = 0 \quad \text{and} \quad \lambda_1^{\mathbf{G}} = \chi v, \quad \lambda_2^{\mathbf{G}} = \lambda_3^{\mathbf{G}} = \lambda_4^{\mathbf{G}} = 0. \quad (13)$$

The important advantage of the system (12) over the original Keller-Segel formulation (1) is that the convective part of this system is purely hyperbolic. Therefore, we do not need to separate the hyperbolic region from the elliptic one in the numerical method.

For the new system (4)-(7), let us formulate first the discontinuous Galerkin method with convective term in the density equation of (4)-(7), approximated by standard upwind technique mentioned above. Let us introduce vector $\mathbf{f} := (u, v)$. In this case the semi-discrete scheme is as followes.
Scheme 2.
Find $(\rho^{DG}, c^{DG}) \in H^1([0,T]) \cap \mathcal{W}^{\rho}_{r_\rho,h} \times \mathcal{W}^{c}_{r_c,h}$ and $(u^{DG}, v^{DG}) \in L^2([0,T]) \cap \mathcal{W}^{u}_{r_u,h} \times \mathcal{W}^{v}_{r_v,h}$ such that:
Equation for ρ :

$$\int_\Omega \rho_t^{DG} w^\rho + \sum_{E\in\mathcal{E}_h} \int_E (\nabla\rho^{DG} - \chi\rho^{DG}\mathbf{f}^{DG})\nabla w^\rho - \sum_{e\in\Gamma_h} \int_e \{\nabla\rho^{DG}\cdot\mathbf{n}_e\}[w^\rho]$$
$$+\varepsilon \sum_{e\in\Gamma_h} \int_e \{\nabla w^\rho\cdot\mathbf{n}_e\}[\rho^{DG}] + \sigma_\rho \sum_{e\in\Gamma_h} \frac{r_\rho^2}{|e|}\int_e [\rho^{DG}][w^\rho] + \sum_{e\in\Gamma_h}\int_e \chi\rho^{DG\uparrow}\mathbf{f}^{DG}\cdot n_e[w^\rho] = 0, \quad \forall w^\rho \in \mathcal{W}^{\rho}_{r_\rho,h} \quad (14)$$

Equation for c :

$$\int_\Omega c_t^{DG} w^c + \sum_{E\in\mathcal{E}_h}\int_E \nabla c^{DG}\nabla w^c - \sum_{e\in\Gamma_h}\int_e \{\nabla c^{DG}\cdot\mathbf{n}_e\}[w^c] + \varepsilon\sum_{e\in\Gamma_h}\int_e \{\nabla w^c\cdot\mathbf{n}_e\}[c^{DG}]$$
$$+\sigma_c \sum_{e\in\Gamma_h}\frac{r_c^2}{|e|}\int_e [c^{DG}][w^c] + \int_\Omega c^{DG}w^c - \int_\Omega \rho^{DG}w^c = 0, \quad \forall w^c \in \mathcal{W}^{c}_{r_c,h} \quad (15)$$

Equation for u :

$$\int_\Omega u^{DG} w^u + \sum_{E\in\mathcal{E}_h}\int_E c^{DG}(w^u)_x - \sum_{e\in\Gamma_h}\int_e c^{DG\uparrow}\cdot\mathbf{n}_x[w^u]$$
$$-\sum_{e\in\partial\Omega_1}\int_e c^{DG}\cdot\mathbf{n}_x w^u + \sigma_u \sum_{e\in\Gamma_h\cup\partial\Omega_1}\frac{r_u^2}{|e|}\int_e [u^{DG}][w^u] = 0, \quad \forall w^u \in \mathcal{W}^{u}_{r_u,h} \quad (16)$$

Equation for v :

$$\int_\Omega v^{DG} w^v + \sum_{E\in\mathcal{E}_h}\int_E c^{DG}(w^v)_y - \sum_{e\in\Gamma_h}\int_e c^{DG\uparrow}\cdot\mathbf{n}_y[w^v]$$

$$-\sum_{e\in\partial\Omega_2}\int_e c^{DG}\cdot\mathbf{n}_y w^v+\sigma_v\sum_{e\in\Gamma_h\cup\partial\Omega_2}\frac{r_v^2}{|e|}\int_e[v^{DG}][w^v]=0,\quad\forall w^v\in\mathcal{W}^v_{r_v,h},\quad(17)$$

and the initial conditions:

$$\int_\Omega\rho^{\mathrm{DG}}(\cdot,0)w^\rho=\int_\Omega\rho(\cdot,0)w^\rho,\quad\int_\Omega c^{\mathrm{DG}}(\cdot,0)w^c=\int_\Omega c(\cdot,0)w^c,$$
$$\int_\Omega u^{\mathrm{DG}}(\cdot,0)w^u=\int_\Omega u(\cdot,0)w^u,\quad\int_\Omega v^{\mathrm{DG}}(\cdot,0)w^v=\int_\Omega v(\cdot,0)w^v.\qquad(18)$$

Finally, the third method that we will consider is the new discontinuous Galerkin schemes developed in [19]. In the same way as it was done in [19], we introduce the following semi-discrete numerical schemes based on three primal discontinuous Galerkin methods, which combine the special treatment of the convective terms:

Scheme 3.

Find $(\rho^{DG},c^{DG})\in H^1([0,T])\cap\mathcal{W}^\rho_{r_\rho,h}\times\mathcal{W}^c_{r_c,h}$ and $(u^{DG},v^{DG})\in L^2([0,T])\cap\mathcal{W}^u_{r_u,h}\times\mathcal{W}^v_{r_v,h}$ such that:

Equation for ρ :

$$\int_\Omega\rho_t^{DG}w^\rho+\sum_{E\in\mathcal{E}_h}\int_E\nabla\rho^{DG}\nabla w^\rho-\sum_{e\in\Gamma_h}\int_e\{\nabla\rho^{DG}\cdot\mathbf{n}_e\}[w^\rho]+\varepsilon\sum_{e\in\Gamma_h}\int_e\{\nabla w^\rho\cdot\mathbf{n}_e\}[\rho^{DG}]$$
$$+\sigma_\rho\sum_{e\in\Gamma_h}\frac{r_\rho^2}{|e|}\int_e[\rho^{DG}][w^\rho]-\sum_{E\in\mathcal{E}_h}\int_E\chi\rho^{DG}u^{DG}(w^\rho)_x+\sum_{e\in\Gamma_h}\int_e(\chi\rho^{DG}u^{DG})^*\cdot\mathbf{n}_x[w^\rho]$$
$$-\sum_{E\in\mathcal{E}_h}\int_E\chi\rho^{DG}v^{DG}(w^\rho)_y+\sum_{e\in\Gamma_h}\int_e(\chi\rho^{DG}v^{DG})^*\cdot\mathbf{n}_y[w^\rho]=0,\quad\forall w^\rho\in\mathcal{W}^\rho_{r_\rho,h}\qquad(19)$$

Equation for c :

$$\int_\Omega c_t^{DG}w^c+\sum_{E\in\mathcal{E}_h}\int_E\nabla c^{DG}\nabla w^c-\sum_{e\in\Gamma_h}\int_e\{\nabla c^{DG}\cdot\mathbf{n}_e\}[w^c]$$
$$+\varepsilon\sum_{e\in\Gamma_h}\int_e\{\nabla w^c\cdot\mathbf{n}_e\}[c^{DG}]+\sigma_c\sum_{e\in\Gamma_h}\frac{r_c^2}{|e|}\int_e[c^{DG}][w^c]+\int_\Omega c^{DG}w^c-\int_\Omega\rho^{DG}w^c=0,\quad\forall w^c\in\mathcal{W}^c_{r_c,h}\qquad(20)$$

Equation for u :

$$\int_\Omega u^{DG}w^u+\sum_{E\in\mathcal{E}_h}\int_E c^{DG}(w^u)_x+\sum_{e\in\Gamma_h}\int_e(-c^{DG})^*_u\cdot\mathbf{n}_x[w^u]$$
$$-\sum_{e\in\partial\Omega_1}\int_e c^{DG}\cdot\mathbf{n}_x w^u+\sigma_u\sum_{e\in\Gamma_h\cup\partial\Omega_1}\frac{r_u^2}{|e|}\int_e[u^{DG}][w^u]=0,\quad\forall w^u\in\mathcal{W}^u_{r_u,h}\quad(21)$$

Equation for v :

$$\int\limits_{\Omega} v^{DG} w^v + \sum_{E\in\mathcal{E}_h} \int\limits_{E} c^{DG}(w^v)_y + \sum_{e\in\Gamma_h} \int\limits_{e} (-c^{DG})^*_v \cdot \mathbf{n}_y [w^v]$$
$$- \sum_{e\in\partial\Omega_2} \int\limits_{e} c^{DG}\cdot\mathbf{n}_y w^v + \sigma_v \sum_{e\in\Gamma_h\cup\partial\Omega_2} \frac{r_v^2}{|e|} \int\limits_{e} [v^{DG}][w^v] = 0, \quad \forall w^v \in \mathcal{W}^v_{r_v,h}, \quad (22)$$

and subject to the initial conditions (18).

To approximate the convective terms in (19) and (21)–(22), we use the central-upwind fluxes developed in ([29,27]):

$$(\chi\rho^{DG}u^{DG})^* = \frac{a^{\text{out}}(\chi\rho^{DG}u^{DG})|^{El_1}_e - a^{\text{in}}(\chi\rho^{DG}u^{DG})|^{El_2}_e}{a^{\text{out}}-a^{\text{in}}} - \frac{a^{\text{out}}a^{\text{in}}}{a^{\text{out}}-a^{\text{in}}}[\rho^{DG}], \quad (23)$$

$$(\chi\rho^{DG}v^{DG})^* = \frac{b^{\text{out}}(\chi\rho^{DG}v^{DG})|^{El_1}_e - b^{\text{in}}(\chi\rho^{DG}v^{DG})|^{El_2}_e}{b^{\text{out}}-b^{\text{in}}} - \frac{b^{\text{out}}b^{\text{in}}}{b^{\text{out}}-b^{\text{in}}}[\rho^{DG}], \quad (24)$$

$$(-c^{DG})^*_u = -\frac{a^{\text{out}}(c^{DG})|^{El_1}_e - a^{\text{in}}(c^{DG})|^{El_2}_e}{a^{\text{out}}-a^{\text{in}}} - \frac{a^{\text{out}}a^{\text{in}}}{a^{\text{out}}-a^{\text{in}}}[u^{DG}], \quad (25)$$

$$(-c^{DG})^*_v = -\frac{b^{\text{out}}(c^{DG})^{El_1} - b^{\text{in}}(c^{DG})|^{El_2}_e}{b^{\text{out}}-b^{\text{in}}} - \frac{b^{\text{out}}b^{\text{in}}}{b^{\text{out}}-b^{\text{in}}}[v^{DG}]. \quad (26)$$

Here, a^{out}, a^{in}, b^{out}, and b^{in} are the one-sided local speeds in the x- and y-directions. Since the convective part of the system (4)–(7) is hyperbolic, these speeds can be estimated using the largest and the smallest eigenvalues of the Jacobian $\frac{\partial\mathbf{F}}{\partial\mathbf{Q}}$ and $\frac{\partial\mathbf{G}}{\partial\mathbf{Q}}$ (see (13)):

$$a^{\text{out}} = \max\left((\chi u^{DG})|^{El_1}_e, (\chi u^{DG})|^{El_2}_e, 0\right), \quad a^{\text{in}} = \min\left((\chi u^{DG})|^{El_1}_e, (\chi u^{DG})|^{El_2}_e, 0\right),$$
$$b^{\text{out}} = \max\left((\chi v^{DG})|^{El_1}_e, (\chi v^{DG})|^{El_2}_e, 0\right), \quad b^{\text{in}} = \min\left((\chi v^{DG})|^{El_1}_e, (\chi v^{DG})|^{El_2}_e, 0\right). \quad (27)$$

Remark. If $a^{\text{out}} - a^{\text{in}} = 0$ at a certain element edge e, we set

$$(\chi\rho^{DG}u^{DG})^* = \frac{(\chi\rho^{DG}u^{DG})|^{El_1}_e + (\chi\rho^{DG}u^{DG})|^{El_2}_e}{2}, \quad (28)$$
$$(\chi\rho^{DG}v^{DG})^* = \frac{(\chi\rho^{DG}v^{DG})|^{El_1}_e + (\chi\rho^{DG}v^{DG})|^{El_2}_e}{2}$$

$$(-c^{DG})^*_u = -\frac{(c^{DG})|^{El_1}_e + (c^{DG})|^{El_2}_e}{2}, \quad (-c^{DG})^*_v = -\frac{(c^{DG})|^{El_1}_e + (c^{DG})|^{El_2}_e}{2}, \quad (29)$$

there.

Let us briefly recall what was proved in [19] for the scheme (19)-(27). We

showed that the scheme (19)-(27) is consistent and we obtained the following hp-error estimates in the assumption that the true solution of (4)-(7) is bounded. We denote by ρ^{DG} and c^{DG} the solution of the (19)-(27).

Assume that:

- For the h- analysis:
  Let the solution of (4)–(7) belongs to $H^{s_1}([0,T]) \cap H^{s_2}(\Omega)$, where $s_1 > 3/2$ and $s_2 \geq 3$.
- For the r- analysis (with respect to the polynomial degree):
  Let the solution of (4)–(7) belongs to $H^{s_1}([0,T]) \cap H^{s_2}(\Omega)$, where $s_1 > 3/2$ and $s_2 \geq 5$.

Remark: We would like to note that the above assumptions make sense, since the solution of the Keller-Segel system (1) is very regular before blow-up time.

Theorem 1 *($L^2(H^1)$ and $L^\infty(L^2)$ error estimates). Let the solution ρ, c, u and v of the Keller-Segel system (4)-(7) satisfy the assumption stated in (3). Furthermore, we assume that penalty parameters $\sigma_\rho, \sigma_c, \sigma_u, \sigma_v$ are sufficiently large. Then there exists constants C_ρ and C_c, independent of h and r, such that*

$$\left\|\rho^{DG}-\rho\right\|_{L^\infty([0,T];L^2(\Omega))}+|||\nabla(\rho^{DG}-\rho)|||_{L^2([0,T];L^2(\Omega))}+\left(\int_0^T \sum_{e\in\Gamma_h}\frac{r_\rho^2}{|e|}\left\|[\rho^{DG}-\rho]\right\|_{0,e}^2\right)^{\frac{1}{2}}$$

$$\leq C_\rho\left(\frac{h^{\min(r_\rho+1,s_\rho)-1}}{r_\rho^{s_\rho-2}}+\frac{h^{\min(r_c+1,s_c)-1}}{r_c^{s_c-2}}+\frac{h^{\min(r_u+1,s_u)-1}}{r_u^{s_u-2}}+\frac{h^{\min(r_v+1,s_v)-1}}{r_v^{s_v-2}}\right)$$

$$\left\|c^{DG}-c\right\|_{L^\infty([0,T];L^2(\Omega))}+|||\nabla(c^{DG}-c)|||_{L^2([0,T];L^2(\Omega))}+\left(\int_0^T \sum_{e\in\Gamma_h}\frac{r_c^2}{|e|}\left\|[c^{DG}-c]\right\|_{0,e}^2\right)^{\frac{1}{2}}$$

$$\leq C_c\left(\frac{h^{\min(r_\rho+1,s_\rho)-1}}{r_\rho^{s_\rho-2}}+\frac{h^{\min(r_c+1,s_c)-1}}{r_c^{s_c-2}}+\frac{h^{\min(r_u+1,s_u)-1}}{r_u^{s_u-2}}+\frac{h^{\min(r_v+1,s_v)-1}}{r_v^{s_v-2}}\right),$$

where $(r_\rho, r_c, r_u, r_v) \geq 2$.

In the same paper, we also showed that the blow up time of the exact solution is bounded from above by the blow up time of the solution of the discontinuous Galerkin schemes (19)-(27).

4 Comparison of the discontinuous Galerkin methods applied to the Keller-Segel chemotaxis model

In this section, we demonstrate the performance of the discontinuous Galerkin schemes introduced in Section (3) for the classical Keller-Segel model. In all our

tests, we used third order SSP Runge-Kutta method for the time discretization [24]. We did not apply slope limiter techniques in the experiments.

Let us consider the following initial boundary value problem for the Keller-Segel system, with chemotactic sensitivity $\chi = 1$ and the radially symmetric bell-shaped initial data,

$$\rho(x, y, 0) = 1200e^{-120(x^2+y^2)}, \quad c(x, y, 0) = 600e^{-60(x^2+y^2)} \tag{30}$$

According to the results in [25,26], both components ρ and c of the solution are expected to blow up at the origin in finite time. This situation is especially challenging, since capturing blowing up solution with shrinking support is extremely hard.

In all experiments we consider fixed mesh with $\Delta x = \Delta y = 1/51$. We use quadratic and cubic discontinuous polynomial approximations $r = 2$ and $r = 3$.

First, let us consider the direct application of the discontinuous Galerkin methods to the original formulation of the Keller-Segel model (see scheme (9)-(10)).

As it was observed in [19], the blow up time t_b for the Keller-Segel problem with initial conditions (30) is $t_b \leq 1.21 \cdot 10^{-4}$. Figure (1), quadratic polynomial approximation is used, shows the solution at time before blow up. Even at early times, the solution shows severe numerical instabilities. On Figure (1) (bottom) it can be seen that the top of the solution splits into two parts. The same severe numerical instabilities can be observed on the figures (2), where a cubic discontinuous polynomial approximation is used.

Next, we consider application of the discontinuous Galerkin methods with the standard upwind fluxes for the reformulated Keller-Segel system (see scheme (14)-(17)). We can see from the Figure (3) that the negative values appeared in the solution even before the blow up time. At the time near the blow up time, see Figure (3) (right, top)- Figure (3) (bottom), the solution shows oscillations. Compared to the results obtained by scheme (9)-(10), these oscillations are not so severe and are now related to the numerical approximations of the convective terms: the numerical fluxes in scheme (14)-(17) ("standard" upwind numerical fluxes) are based on the approximate of the Riemann problem solver, which is not available for the system under consideration. As a consequence, Scheme 2 does not reconstruct the solution accurately. Similar results are shown on Figure (4), where the cubic polynomial approximations are used.

Finally, Figure (5) shows the performance of the new discontinuous Galerkin methods (19)-(27). Again we consider quadratic and cubic discontinuous polynomial approximations respectively. The obtained numerical solution has no

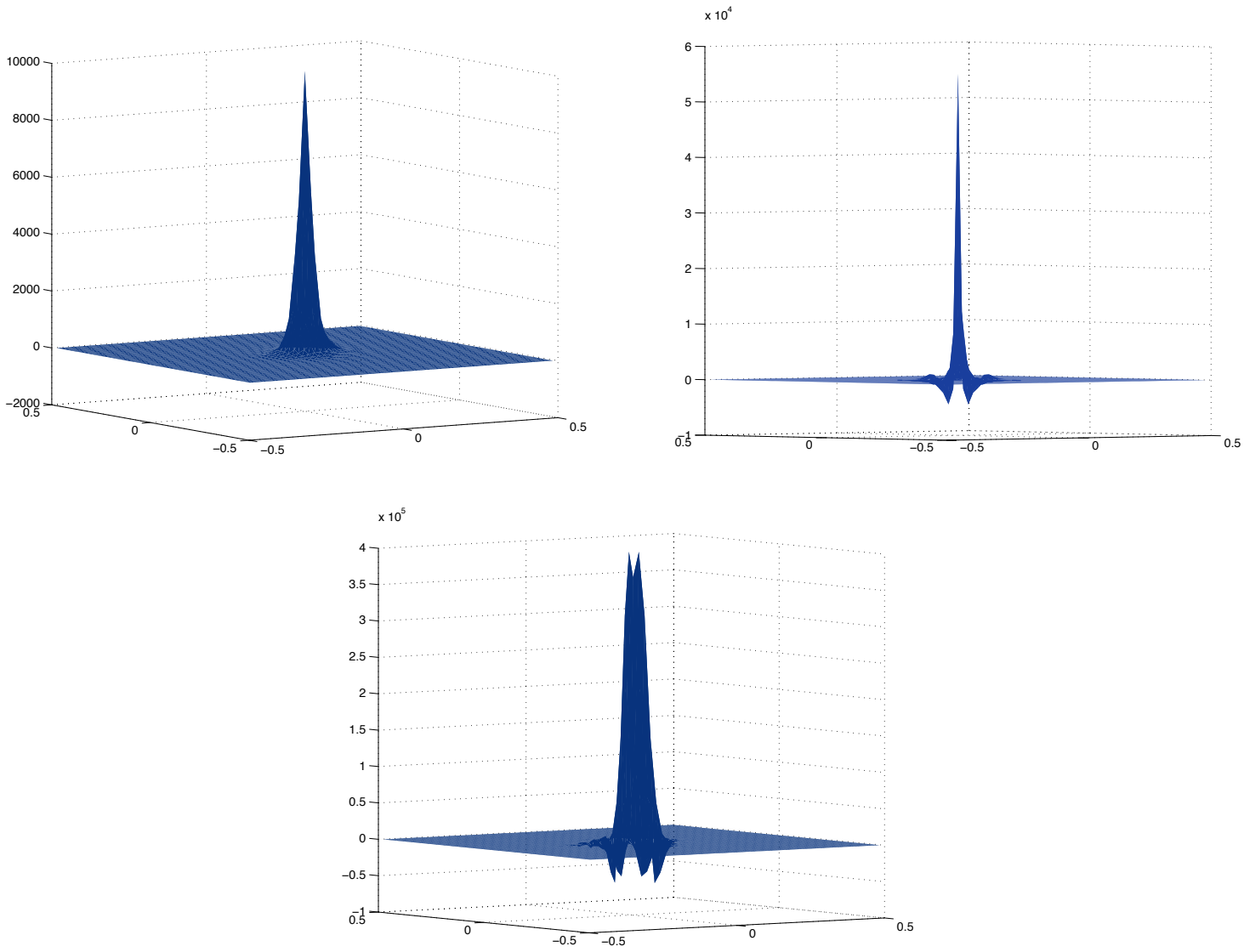

Fig. 1. original formulation: $h = 1/51, r = 2$; $t = 1.5 \cdot 10^{-5}$ (left, top), $t = 3.0 \cdot 10^{-5}$ (right, top) and $t = 4.5 \cdot 10^{-5}$ (bottom)

negative values and is oscillation free.

5 Haptotaxis Model of the Tumor Invasion into Healthy Tissue

In this section, we will consider the application of the new discontinuous Galerkin methods (see scheme (19)-(27) for the Keller-Segel model) to the simulation of the haptotaxis model of tumor invasion into healthy tissue, proposed in [3], [9,10].

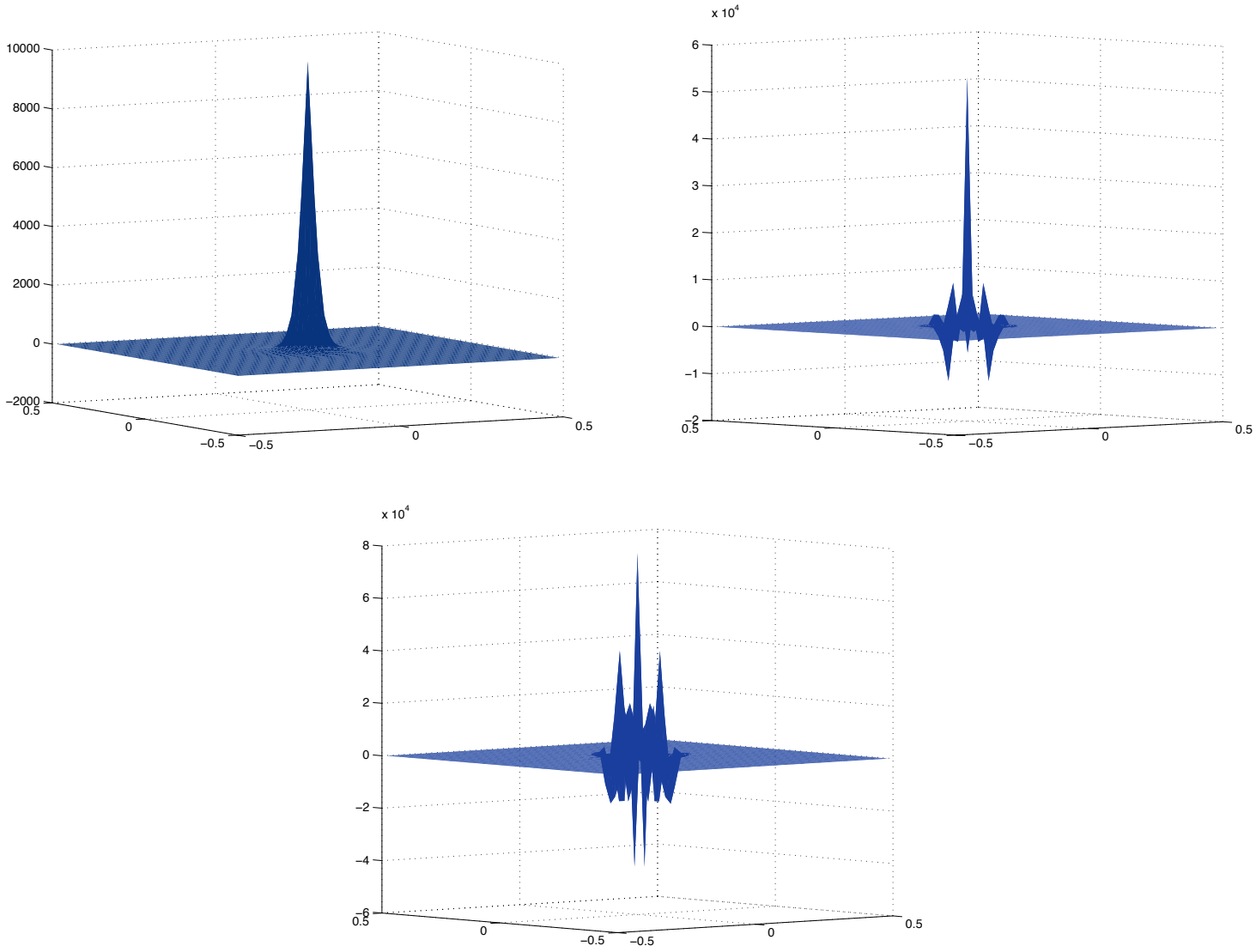

Fig. 2. $h = 1/51, r = 3 : t = 1.5 \cdot 10^{-5}$ (top, left), $t = 3.0 \cdot 10^{-5}$ (top,right), $t = 3.6 \cdot 10^{-5}$ (bottom)

The term *haptotaxis* originated with S.B. Carter in 1965: "... the movement of a cell is controlled by the relative strengths of its peripheral adhesions, and that movements directed in this way, together with the influence of patterns of adhesion on cell shape are responsible for the arrangement of cells into complex and ordered tissues" [9]. Cell movement in inflammation, tumor invasion, and other migrations are the result of haptotactic responses of cells to differential adhesion strengths [9,10].

The development of a primary solid tumor (e.g., a carcinoma) begins with a single normal cell becoming transformed, as a result of mutations in certain key genes. The next stage is that the primary tumor induces the formation of

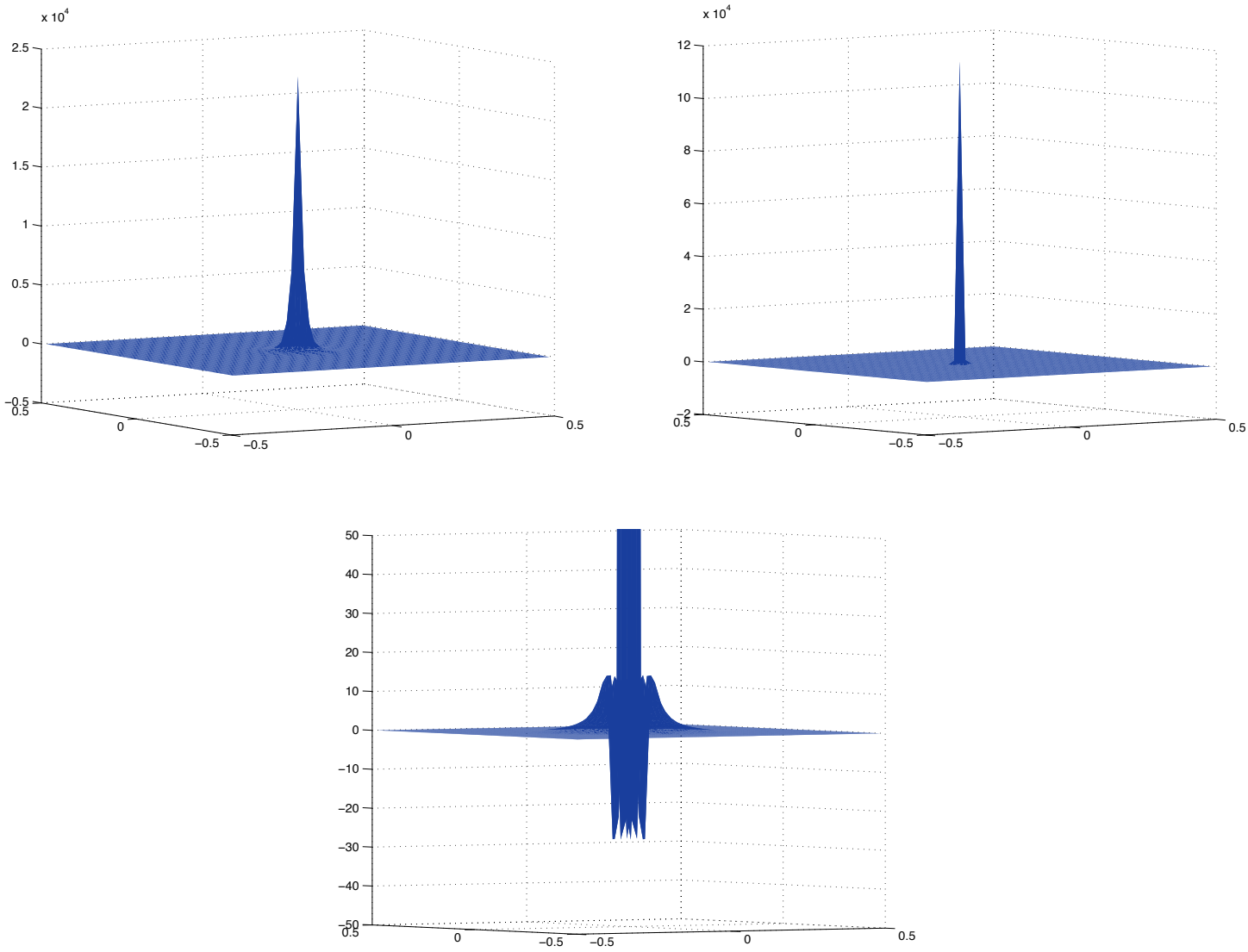

Fig. 3. $h = 1/51, r = 2 : t = 6.0 \cdot 10^{-5}$ (left, top), t near $t_b = 1.21 \cdot 10^{-4}$ (right, top), zoom view of the figure on the right (bottom)

a local vascular network and creates its own blood supply. After this stage, the *tumor invasion* occurs: first, cancer cells escape from the primary tumor; second, the cells locally degrade the surrounding tissue and continue migration.

The haptotaxis model of tumor invasion in 2D is the system of the nonlinear convection-reaction-diffusion equations:

$$\rho_t + \nabla \cdot (\chi(c)\rho\nabla c) - d_\rho \Delta\rho + \psi(x,y,w)\rho - \phi(x,y,w)\rho = 0, \tag{31}$$

$$c_t + \alpha(x,y)mc = 0, \tag{32}$$

$$m_t - d_m \Delta m - \delta(x,y)\rho + \beta(x,y)m = 0, \tag{33}$$

$$w_t - d_w \Delta w - \gamma(x,y)c + e(x,y)w + \nu(x,y,\rho)w = 0,, \tag{34}$$

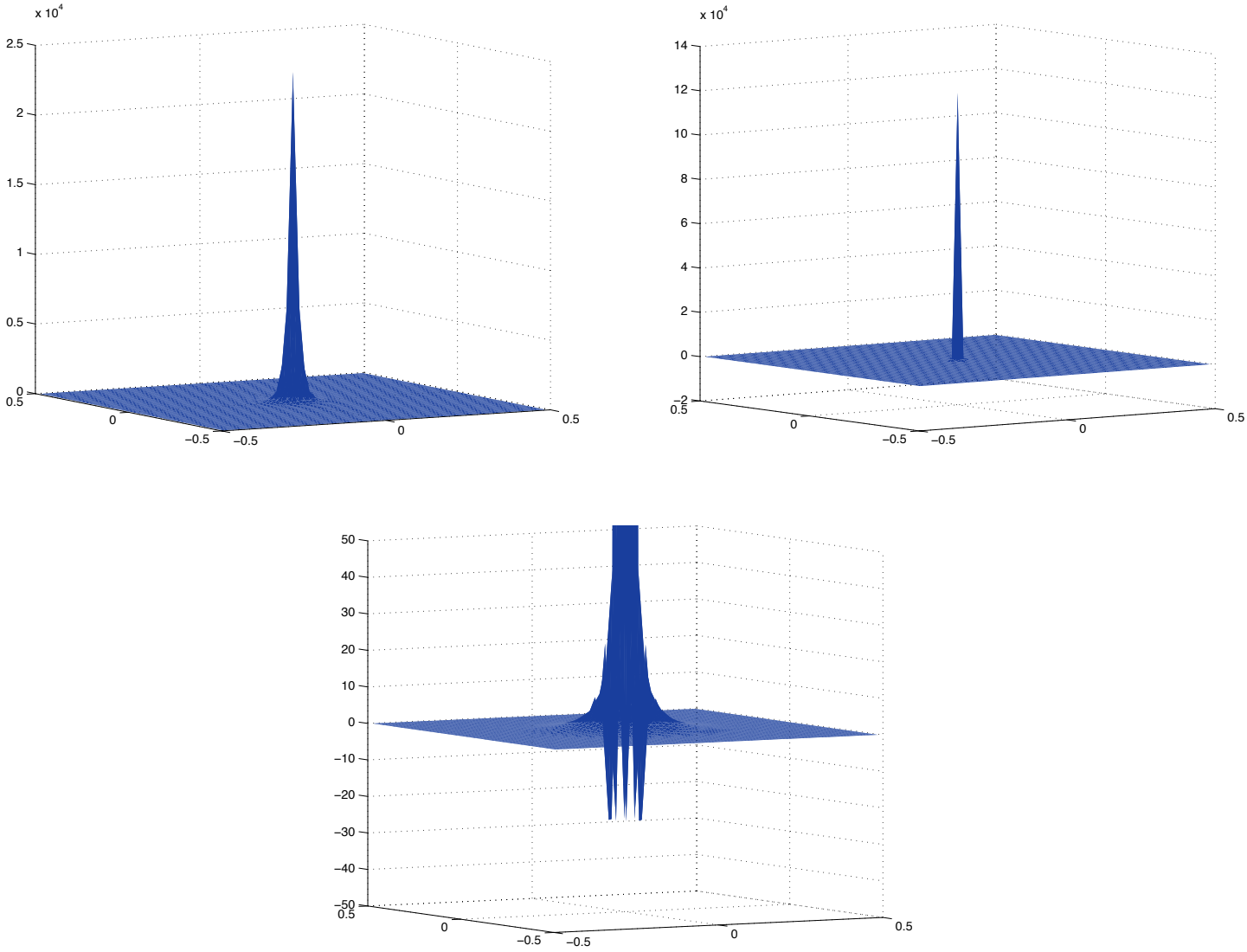

Fig. 4. $h = 1/51, r = 3 : t = 6.0 \cdot 10^{-5}$ (left), t near $t_b = 1.21 \cdot 10^{-4}$ (right), zoom view of the figure on the right (bottom)

subject to the Neumann boundary conditions:

$$\nabla\rho \cdot \mathbf{n} = \nabla c \cdot \mathbf{n} = \nabla m \cdot \mathbf{n} = \nabla w \cdot \mathbf{n} = 0, \quad (x, y) \in \partial\Omega,$$

where we have the following variables in (31)-(34):

- $\rho(x, y, t)$ is the density of tumor cells (cancerous cells)
- $c(x, y, t)$ is the density of extracellular matrix macromolecules
- $m(x, y, t)$ is the concentration of matrix degradative enzyme
- $w(x, y, t)$ is the concentration of the oxygen

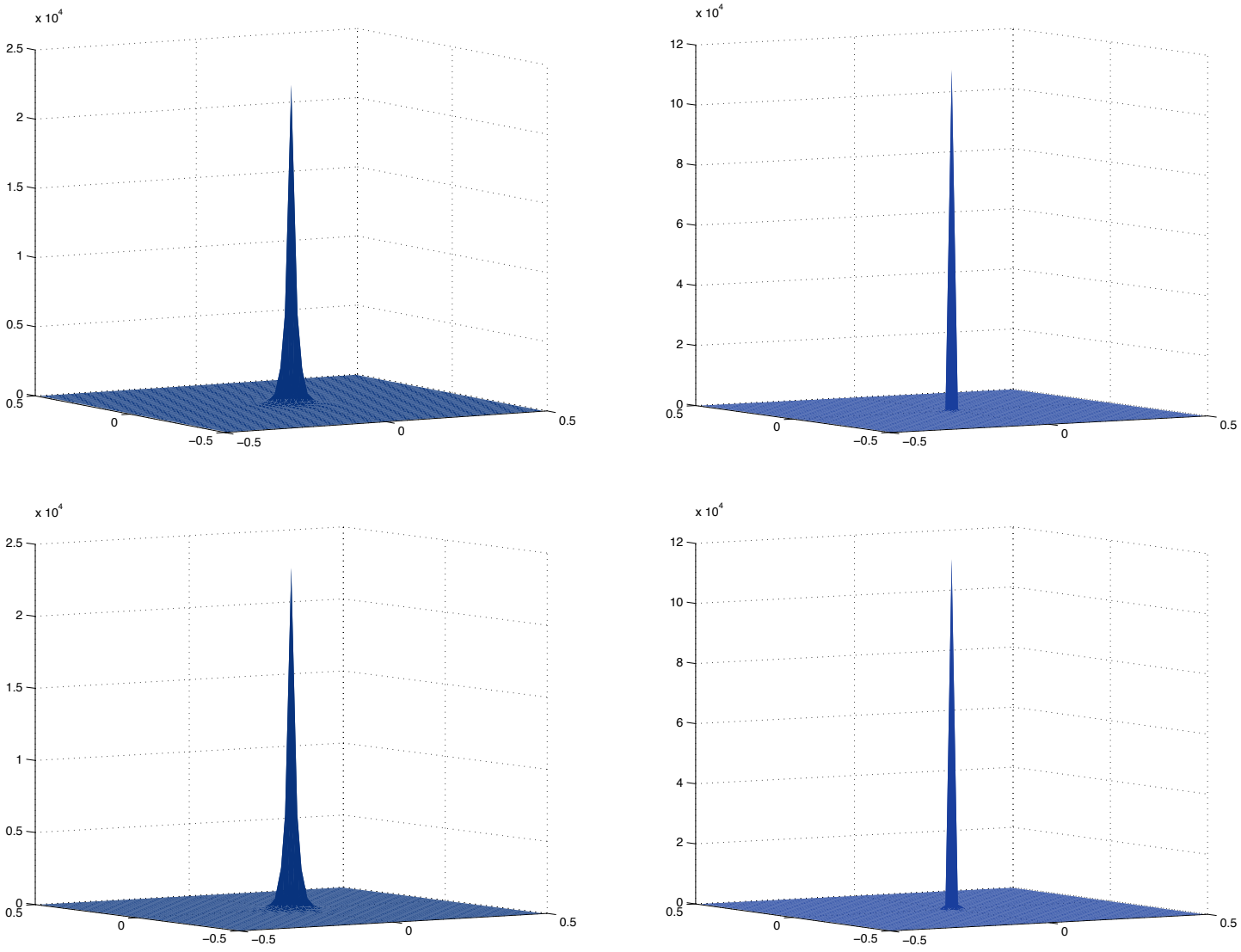

Fig. 5. $h = 1/51, r = 2 : t = 6.0 \cdot 10^{-5}$ (left, top) , t near $t_b = 1.21 \cdot 10^{-4}$ (right, top); $r = 3 : t = 6.0 \cdot 10^{-5}$ (left, bottom) , t near $t_b = 1.21 \cdot 10^{-4}$ (right, bottom)

The rest of the parameters in (31)-(34) will be specified in the numerical experiments below.

Now let us apply the new discontinuous Galerkin schemes to the haptotaxis system (31)-(34). As it was done for the Keller-Segel model (1), we introduce the new variables $u := c_x$ and $v := c_y$. Then the modified haptotaxis system (31)-(34) will be

$$k_1 \mathbf{Q}_t + \mathbf{F}(\mathbf{Q})_x + \mathbf{G}(\mathbf{Q})_y = k_2 \Delta \mathbf{Q} + \mathbf{R}(\mathbf{Q}), \tag{35}$$

where $\mathbf{Q} := (\rho, c, m, w, u, v)^T$, the fluxes are $\mathbf{F}(\mathbf{Q}) := (\chi(c)\rho u, 0, 0, 0, c, 0)^T$ and $\mathbf{G}(\mathbf{Q}) := (\chi(c)\rho v, 0, 0, 0, 0, c)^T$, the reaction term is $\mathbf{R}(\mathbf{Q}) := (-\psi(x, y, w)\rho +$

$\phi(x,y,w)\rho, \quad -\alpha(x,y)mc, \quad \delta(x,y)\rho - \beta(x,y)m, \quad \gamma(x,y)c - \nu(x,y,\rho)w - e(x,y)w, u, v)$,
k_1 is given by

$$k_1 = \begin{cases} 1 \ \text{ for } \mathbf{Q}^{(1)} := \rho \ , \ \mathbf{Q}^{(2)} := c, \ \mathbf{Q}^{(3)} := m, \ \text{and } \mathbf{Q}^{(4)} := w \\ 0 \ \text{ for } \mathbf{Q}^{(5)} := u \text{ and } \mathbf{Q}^{(6)} := v. \end{cases}$$

and k_2 is given by

$$k_2 = \begin{cases} d_\rho \ \text{ for } \mathbf{Q}^{(1)}, \\ d_m \ \mathbf{Q}^{(3)}, \\ d_w \ \mathbf{Q}^{(4)}, \\ 0 \ \text{ for } \mathbf{Q}^{(2)} \ , \ \mathbf{Q}^{(5)} \text{ and } \mathbf{Q}(6). \end{cases}$$

The eigenvalues of the Jacobian $\frac{\partial \mathbf{F}}{\partial \mathbf{Q}}$ and $\frac{\partial \mathbf{G}}{\partial \mathbf{Q}}$ are

$$\lambda_1^{\mathbf{F}} = \chi(c)u, \lambda_2^{\mathbf{F}} = ... = \lambda_6^{\mathbf{F}} = 0 \text{ and } \lambda_1^{\mathbf{G}} = \chi(c)v, \lambda_2^{\mathbf{G}} = ... = \lambda_6^{\mathbf{G}} = 0 \qquad (36)$$

As for the reformulated Keller-Segel model of chemotaxis (12), the convective part of the haptotaxis system (35) is hyperbolic. Thus, the one-sided local speeds can be taken as the largest/smallest eigenvalues of the corresponding Jacobians.

The new discontinuous Galerkin scheme can then be applied to the system (35) in a straightforward manner, similar to the application of the scheme (19)-(27) for the chemotaxis problem.

For the first numerical experiments we consider the following choice of parameters:

$$\begin{gathered} \chi(c) = 0.4, \quad d_\rho = 0.01, \quad \psi(x,y,w) = 0.1, \\ \phi(x,y,w) = \frac{2w}{1+w}, \quad \alpha = 5, \quad d_m = 0.01, \\ \delta(x,y) = 1, \quad \beta(x,y) = 0.01, \quad d_w = 0.1, \\ \gamma(x,y) = 5, \quad \nu(x,y,\rho) = \frac{2\rho}{1+\rho}, \quad e(x,y) = 1. \end{gathered} \qquad (37)$$

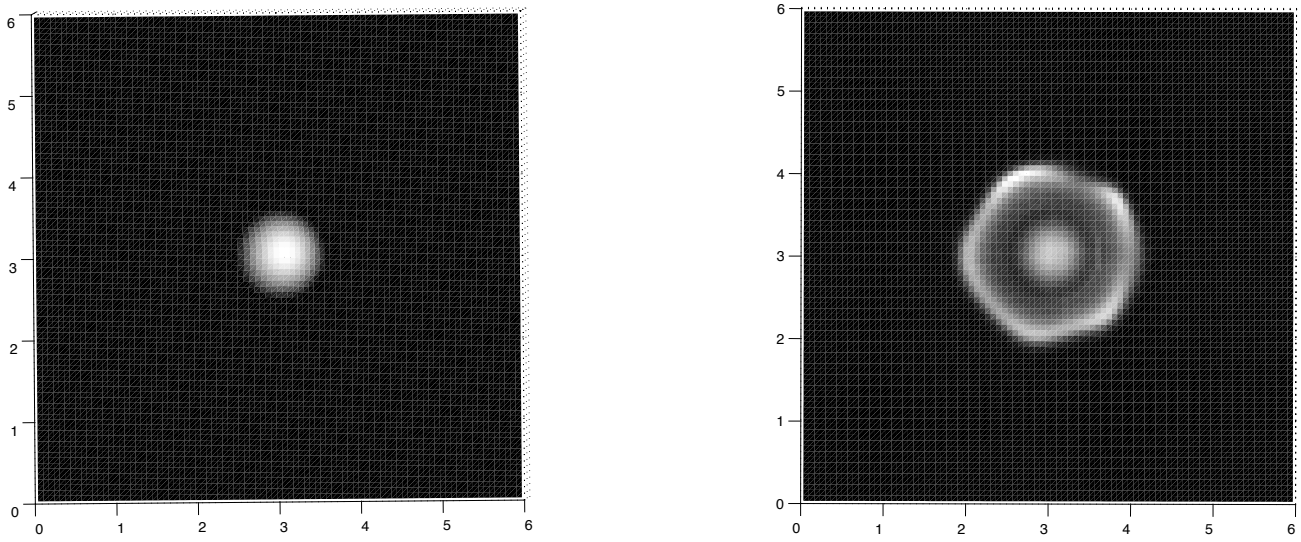

Fig. 6. $h = 1/75, r = 3 : t = 0$ (left), $t = 2.0$ (right)

The initial data are given by

$$\begin{aligned} \rho(x,y,0) &= 5\max\{0.3-(x-3)^2-(y-3)^2, 0\}, \\ c(x,y,0) &= 0.05\cos(\frac{5\pi x^2}{12})\sin(\frac{13\pi y^2}{72}), \\ m(x,y,0) &= \rho(x,y,0), \quad w(x,y,0) = 4c(x,y,0). \end{aligned} \tag{38}$$

We consider uniform mesh with $\Delta x = \Delta y = 1/75$, and we use a cubic discontinuous polynomial approximation. The results are shown on Figures (6)-(9) for the density of the cancerous cell ρ.

The figures show the tumor cells invasion of the tissue at different times. Compared to Keller-Segel chemotaxis model, the solution of the haptotaxis model does not blow-up. The results obtained here are in good agreement with the results reported in [11,39]. This confirms the robustness of the proposed new discontinuous Galerkin method.

Next, we repeat the same experiment with the data stated as before, except we set diffusion coefficient $d_\rho = 0.005$, which is 2 times smaller than in the first experiment. The 3D-view of the results (density ρ) are shown on Figure (10).

In the first and second experiments, the diffusion has caused the cell density to spread out in the domain. But in the second experiment (with lower diffusion coefficient), the cell density profile develops steeper transition fronts and they are more compact.

Acknowledgment: I would like to thank Professor Alexander Kurganov for

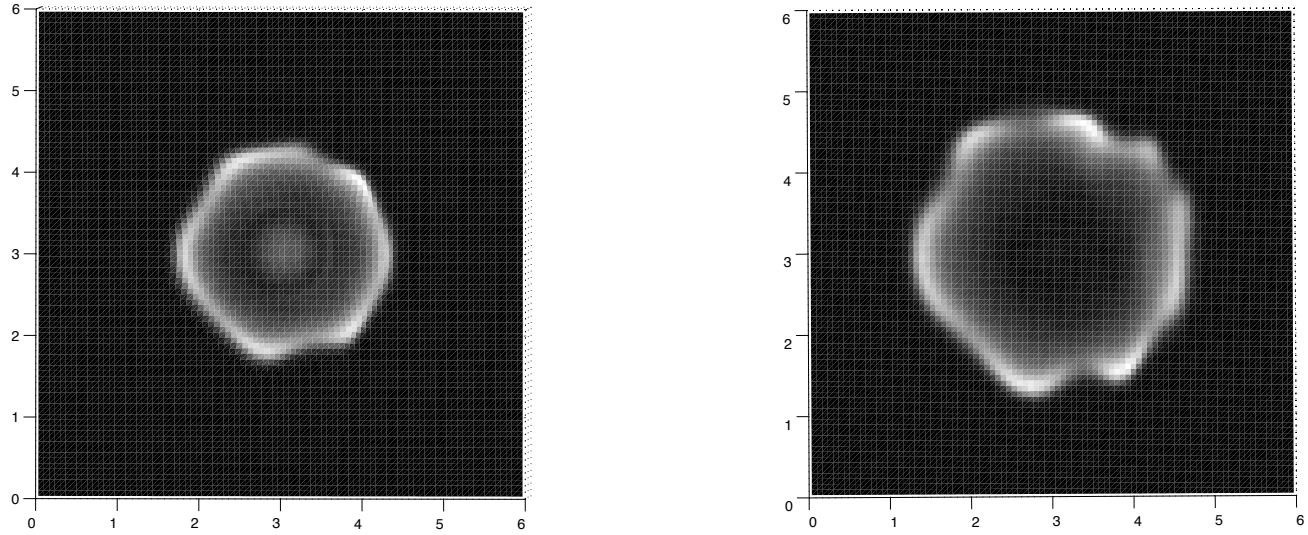

Fig. 7. $h = 1/75, r = 3 : t = 3.0$ (left), $t = 5.0$ (right)

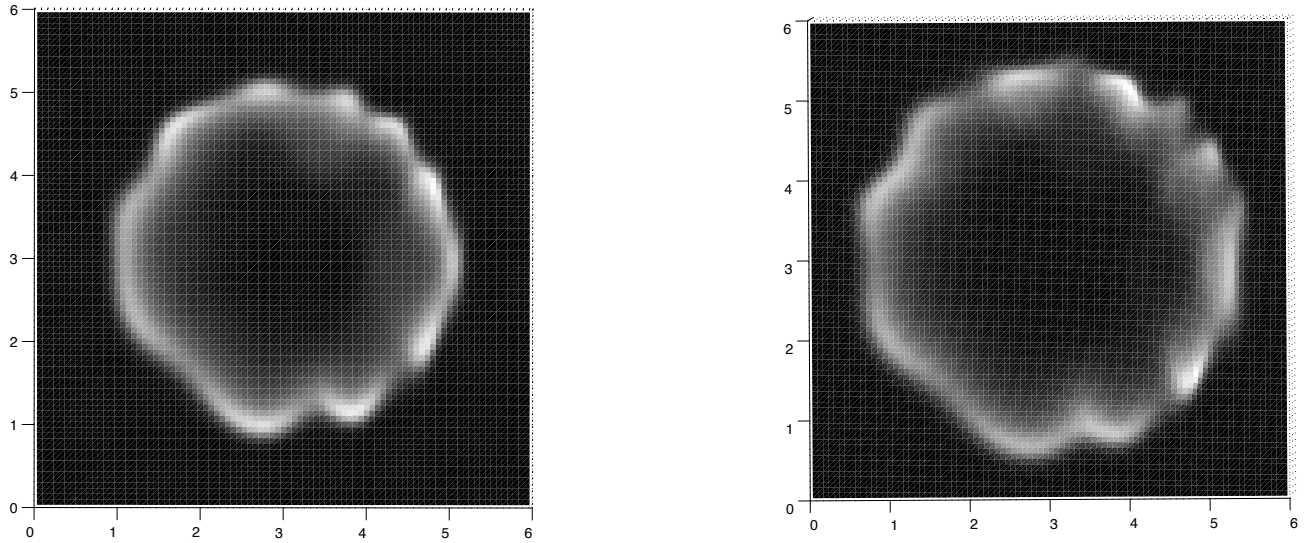

Fig. 8. $h = 1/75, r = 3 : t = 7.0$ (left), $t = 9.0$ (right)

the helpful discussions.

References

[1] J. Adler, *Chemotaxis in bacteria*, Ann. Rev. Biochem., 44 (1975), pp. 341–356.

[2] V. Aizinger, C. Dawson, B. Cockburn, and P. Castillo, *Local discontinuous Galerkin methods for contaminant transport*, Adv. in Water Res., 24 (2000), pp. 73–87.

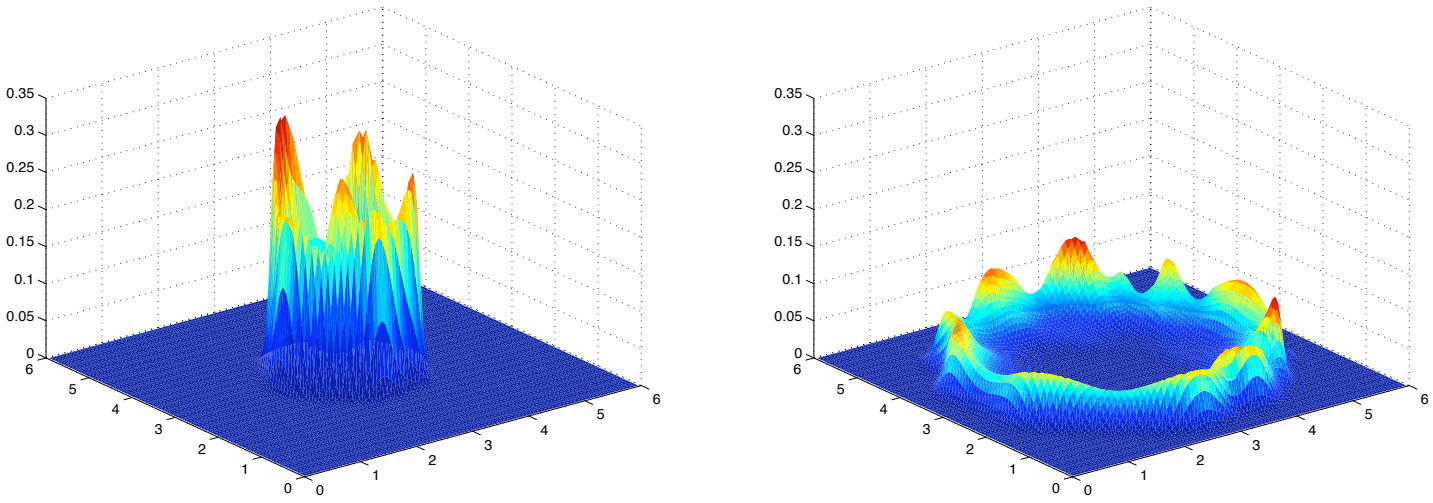

Fig. 9. $h = 1/75, r = 3 : t = 2.0$ (left), $t = 9.0$ (right), diffusion coefficient $d_\rho = 0.01$

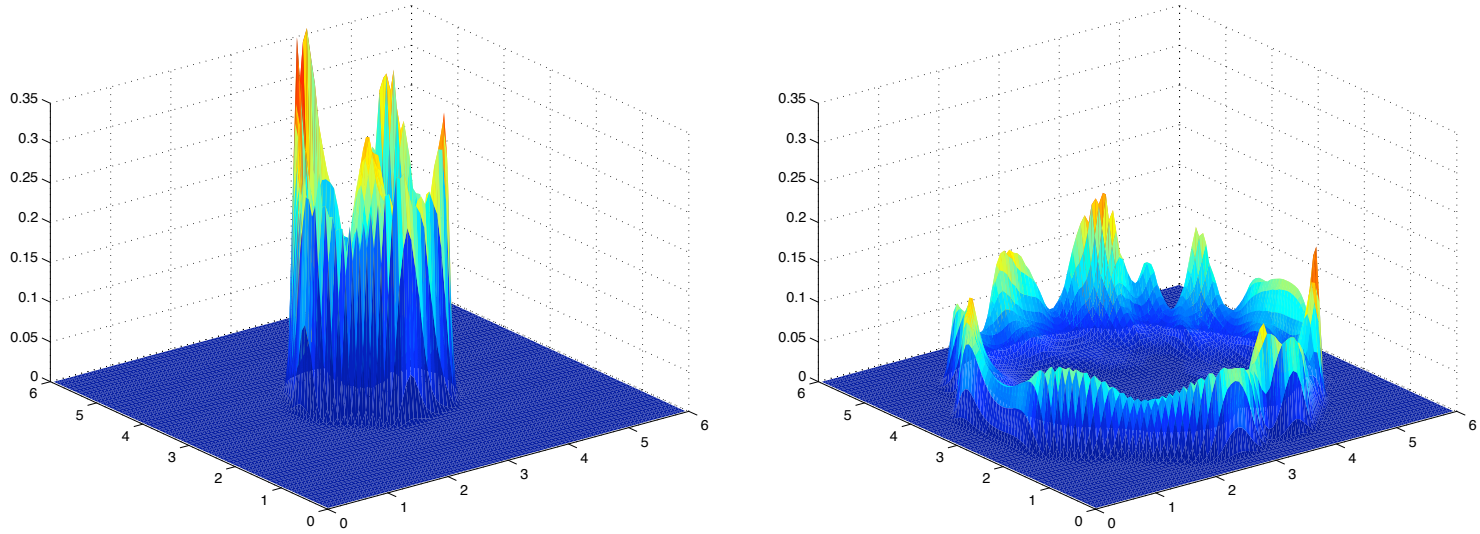

Fig. 10. $h = 1/75, r = 3 : t = 2.0$ (left), $t = 9.0$ (right), diffusion coefficient $d_\rho = 0.005$

[3] A. R. A. Anderson, *A hybrid mathematical model of solid tumour invasion: The importance of cell adhesion*, Math. Med. Biol. IMA J., 22 (2005), pp. 163–186.

[4] D.N. Arnold, *An interior penalty finite element method with discontinuous elements*, SIAM J. Numer. Anal., 19 (1982), pp. 742–760.

[5] G.A. Baker, W.N. Jureidini, and O.A. Karakashian, *Piecewise solenoidal vector fields and the Stokes problem*, SIAM J. Numer. Anal., 27 (1990), pp. 1466–1485.

[6] J.T. Bonner, *The cellular slime molds*, Princeton University Press, Princeton, New Jersey, 2nd ed., 1967.

[7] E.O. Budrene and H.C. Berg, *Complex patterns formed by motile cells of escherichia coli*, Nature, 349 (1991), pp. 630–633.

[8] E.O. Budrene and H.C. Berg, *Dynamics of formation of symmetrical patterns by chemotactic bacteria*, Nature, 376 (1995), pp. 49–53.

[9] S. B. Carter, *Principles of cell motility: The direction of cell movement and cancer invasion*, Nature, 208 (1965), pp. 1183–1187.

[10] S. B. Carter, *Haptotaxis and the mechanism of cell motility*, Nature, 213 (1967), pp. 256–260.

[11] A. Chertock and A. Kurganov, *A positivity preserving central-upwind scheme for chemotaxis and haptotaxis models*, Numer. Math. submitted.

[12] S. Childress and J.K. Percus, *Nonlinear aspects of chemotaxis*, Math. Biosc., 56 (1981), pp. 217–237.

[13] B. Cockburn, G.E. Karniadakis, and C.-W. Shu, eds., *First International Symposium on Discontinuous Galerkin Methods*, vol. 11 of Lecture Notes in Computational Science and Engineering, Springer-Verlag, 2000.

[14] B. Cockburn and C.-W. Shu., *The local discontinuous Galerkin method for convection-diffusion systems*, SIAM J. Numer. Anal., 35 (1998), pp. 2440–2463.

[15] M.H. Cohen and A. Robertson, *Wave propagation in the early stages of aggregation of cellular slime molds*, J. Theor. Biol., 31 (1971), pp. 101–118.

[16] C. Dawson, E. Kubatko, and J. Westerink, *hp Discontinuous Galerkin methods for advection-dominated problems in shallow water*, Comp. Meth. Appl. Mech. Eng. to appear.

[17] C. Dawson, S. Sun, and M.F. Wheeler, *Compatible algorithms for coupled flow and transport*, Comput. Meth. Appl. Mech. Engng, 193 (2004), pp. 2565–2580.

[18] J. Douglas and T. Dupont, *Lecture Notes in Physics*, vol. 58, Springer-Verlag, 1976, ch. Interior penalty procedures for elliptic and parabolic Galerkin methods.

[19] Y. Epshteyn and A. Kurganov, *New Interior Penalty Discontinuous Galerkin Methods for the Keller-Segel Chemotaxis Model*, CNA report, submitted (2007).

[20] Y. Epshteyn and B. Rivière, *Estimation of penalty parameters for symmetric interior penalty Galerkin methods*, Journal of Computational and Applied Mathematics, (2006). doi: 10.1016/j.cam.2006.08.029.

[21] Y. Epshteyn and B. Rivière, *On the solution of incompressible two-phase flow by a p-version discontinuous Galerkin method*, Comm. Numer. Methods Engrg., 22 (2006), pp. 741–751.

[22] F. Filbet, *A finite volume scheme for the Patlak-Keller-Segel chemotaxis model*, Numer. Math., 104 (2006), pp. 457–488.

[23] V. Girault, B. Rivière, and M.F. Wheeler, *A discontinuous Galerkin method with non-overlapping domain decomposition for the Stokes and Navier-Stokes problems*, Math. Comp., 74 (2005), pp. 53–84.

[24] S. Gottlieb, C.-W. Shu, and E. Tadmor, *High order time discretization methods with the strong stability property*, SIAM Review, 43 (2001), pp. 89–112.

[25] D. Horstmann, *From 1970 until now: The Keller-Segel model in chemotaxis and its consequences I*, Jahresber. DMV, 105 (2003), pp. 103–165.

[26] D. Horstmann, *From 1970 until now: The Keller-Segel model in chemotaxis and its consequences II*, Jahresber. DMV, 106 (2004), pp. 51–69.

[27] O. Karakashian and F. Pascal, *A posteriori error estimates for a discontinuous Galerkin approximation of second order elliptic problems*, SIAM J. Numer. Anal, 41 (2003), pp. 2374–2399.

[28] A. Kurganov and C.-T. Lin, *On the reduction of numerical dissipation in central-upwind schemes*, Commun. Comput. Phys., 2 (2007), pp. 141–163.

[29] A. Kurganov, S. Noelle, and G. Petrova, *Semi-discrete central-upwind schemes for hyperbolic conservation laws and Hamilton-Jacobi equations*, SIAM J. Sci. Comput., 23 (2001), pp. 707–740.

[30] A. Kurganov and G. Petrova, *Central-upwind schemes on triangular grids for hyperbolic systems of conservation laws*, Numer. Methods Partial Differential Equations, 21 (2005), pp. 536–552.

[31] A. Marrocco, *2D simulation of chemotaxis bacteria aggregation*, M2AN Math. Model. Numer. Anal., 37 (2003), pp. 617–630.

[32] L.M. Prescott, J.P. Harley, and D.A. Klein, *Microbiology*, Wm. C. Brown Publishers, Chicago, London, 3rd ed., 1996.

[33] J. Proft and B. Rivière, *Analytical and numerical study of diffusive fluxes for transport equations with near-degenerate coefficients*, University of Pittsburgh report, submitted (2007).

[34] J. Qiu, B. Khoo, and C.W. Shu, *A numerical study for the performance of the Runge-Kutta discontinuous Galerkin method based on different numerical fluxes*, 212 (2005).

[35] B. Rivière, M.F. Wheeler, and V. Girault., *A priori error estimates for finite element methods based on discontinuous approximation spaces for elliptic problems*, SIAM J. Numer. Anal., 39 (2001), pp. 902–931.

[36] S. Sun and M.F. Wheeler, *Symmetric and nonsymmetric discontinuous Galerkin methods for reactive transport in porous media*, SIAM J. Numer. Anal., 43 (2005), pp. 195–219.

[37] R. Tyson, S.R. Lubkin, and J.D. Murray, *A minimal mechanism for bacterial pattern formation*, Proc. Roy. Soc. Lond. B, 266 (1999), pp. 299–304.

[38] R. Tyson, L.G. Stern, and R.J. LeVeque, *Fractional step methods applied to a chemotaxis model*, J. Math. Biol., 41 (2000), pp. 455–475.

[39] C. Walker and G.F. Webb, *Global Existence of classical solutions for a haptotaxis model*, preprint.